JOURNAL OF SOLID STATE CHEMISTRY **134,** 349–355 (1997)
ARTICLE NO. SC977578

# Oxyfluorinated Open Framework Compounds

## XIX. Hydrothermal Synthesis, Structure Determination, and Magnetic Properties of the Iron (III) Phosphate $[Fe_3(PO_4)_3F_2, (CH_3NH_3)_2, H_2O]$: Comparison with the Isostructural Oxyfluorinated Gallophosphate ULM-4

M. Cavellec,* C. Egger,* J. Linares,† M. Nogues,† F. Varret,† and G. Férey*,[1]

*Institut Lavoisier, IREM UMR C173, Université de Versailles-St Quentin-en-Yvelines, 45, avenue des Etats-Unis, 78035 Versailles Cedex, France; and †Laboratoire de magnétisme et d'optique de Versailles, Université de Versailles-St Quentin-en-Yvelines, 45, avenue des Etats-Unis, 78035 Versailles Cedex, France

Received July 25, 1997; accepted July 30, 1997

**$[Fe_3(PO_4)_3F_2, (CH_3NH_3)_2, H_2O]$ or ULM-4 is a new iron phosphate with an open framework synthesized by a hydrothermal method (72 h at 453 K). The structure was solved by X-ray diffraction on single crystal. ULM-4 crystallizes in the monoclinic system (space group $P2_1/n$ (no. 14)) with cell parameters at 293 K: $a = 8.8494(1)$, $b = 10.3728(1)$, $c = 16.9471(1)$ Å, $\beta = 92.869°(1)$, $V = 1553.68$ (2) Å$^3$, $Z = 4$. Its structure was refined to $R_1(F_0) = 0.0276$, $wR_2(F_0^2) = 0.0741$ (5033 independent reflections with $I > 2\sigma(I)$). This compound is isostructural with the oxyfluorinated gallophosphate ULM-4. Its three-dimensional framework is built up from corner-sharing hexameric units, thus delimiting 10-membered channels along [010] in which methylamine and water molecules are inserted. It also exhibits 8-membered channels along [100]. A phase transition occurs at 265 K. This new compound exhibits an antiferromagnetic behavior below 25(1) K. Mössbauer spectrometry confirms the crystallographic results.** 

## INTRODUCTION

In the past few years, much research has been devoted to the hydrothermal synthesis of new 3*d* transition metals (Mo, V, Co) open-framework phosphates. Most of these compounds (1–3) are mixed organic–inorganic compounds in which amines act as templating agents.

Since 1994, we synthesized several open framework iron phosphates as ULM-10 (4), ULM-12 (5), and ULM-15 (6). This research originated from the hypothesis for a mechanism of formation of open framework alumino and gallophosphates (first ULM-*n* phases) proposed by Férey (7). This hypothesis was independent of the nature of the metallic cation and predicted the synthesis of 3*d* metallophosphates.

Up to now, we have succeeded in synthesizing new *V*-based (ULM-7 (8)) and *Fe*-based ULM compounds (ULM-12, 15, 19), and also fluorinated iron phosphates isostructural with aluminium or gallium based ULM phases. This last point concerns ULM-3 (9), ULM-11 (10), and the title compound ULM-4. Very recently, we were also informed of the existence of new iron oxyphosphates (11, 12).

This paper describes the synthesis, crystal structure, and magnetic properties (susceptibility measurements and Mössbauer spectroscopy) of ULM-4 or $[Fe_3(PO_4)_3F_2, (CH_3NH_3)_2, H_2O]$.

## EXPERIMENTAL

### 1. Synthesis

$[Fe_3(PO_4)_3F_2, (CH_3NH_3)_2, H_2O]$ or ULM-4 was hydrothermally synthesized from a mixture composed of $Fe_2O_3$ (Aldrich, 99%+), $H_3PO_4$ (Prolabo RP Normapur, 85%, 7.5M), HF (Prolabo RP Normapur, 48%, 4.6M), methylamine (Aldrich, 40 wt%), and water in the molar ratios 1.5 : 3 : 2 : 3.4 : 120. The mixture was sealed in a Teflon-lined stainless-steel-autoclave at 180°C for 72 h. The initial pH was 2, the final pH level reached 3. The resulting product was filtered off, washed with distilled water, and dried in air at room temperature. It consists of a mixture of thick yellow transparent platelets (yield 10%) and unreacted $Fe_2O_3$.

TGA measurements were performed under $O_2$ atmosphere using a TA-Instrument type 2050 analyzer. The heating rate was 5°C/min from 30 to 550°C.

DSC measurements were performed using a TA-Instrument 2010 apparatus in the temperature range 77–300 K with a heating rate of 5°C/min.

[1] To whom correspondence should be addressed.



0022-4596/97 $25.00

**TABLE 1**
**Crystal Data and Structure Refinement for $[Fe_3(PO_4)_3F_2, (CH_3NH_3)_2, H_2O]$**

| | |
|---|---|
| Empirical formula | $[Fe_3(PO_4)_3F_2, (CH_3NH_3)_2, H_2O]$ |
| Formula weight | 570.60 g/mol |
| Temperature | 303(2) K |
| Wavelength | 0.71073 Å (Mo) |
| Crystal system | monoclinic |
| Space group | $p2_1/n$ (no. 14) |
| Unit-cell dimensions | $a = 8.8494(1)$ Å |
| | $b = 10.3728(1)$ Å $\beta = 92.869(1)^\circ$ |
| | $c = 16.9471(1)$ Å |
| Volume, $Z$ | 1553.68(2) Å$^3$, 4 |
| Density (calculated) | 2.439 g/cm$^3$ |
| Absorption coefficient | 31.65 cm$^{-1}$ |
| Absorption correction | peculiar to CCD detector (SADABS) |
| $F(000)$ | 1132 |
| Crystal size | $0.36 \times 0.2 \times 0.08$ mm (fragment) |
| Theta range for data collection | 3.80 to 32.36° |
| Limiting indices | $-9 \le h \le 13$, $-15 \le k \le 13$, |
| | $-20 \le l \le 25$ |
| Reflections collected | 12433 |
| Independent reflections | 5033 [$R$(int) = 0.0289] |
| Refinement method | Full-matrix least-squares on $F^2$ |
| Data/restraints/parameters | 5033/0/232 |
| Goodness-of-fit on $F^2$ | 0.979 |
| Final $R$ indices [$I > 2\sigma(I)$] | $R_1(F_0) = 0.0276$, w$R_2(F_0^2) = 0.0741$ |
| $R$ indices (all data) | $R_1(F_0) = 0.0299$, w$R_2(F_0^2) = 0.0757$ |
| Extinction coefficient | 0.0053(4) |
| Largest differential peak and hole | 0.808 and $-1.032$ e$^-$ Å$^{-3}$ |

## 2. Structure Determination

A suitable single crystal was isolated for data collection on a Siemens-type SMART three-circle diffractometer equipped with a CCD bidimensional detector. Conditions of data measurements are summarized in Table 1.

The structure of $[Fe_3(PO_4)_3F_2, (CH_3NH_3)_2, H_2O]$ was solved by the direct methods using the TREF option of the SHELXTL program. The six heaviest atoms (3 Fe + 3 P) were first located. The remaining atoms (O, N, C) were deduced from Fourier-difference calculations of the SHELXTL program. Fluorine atoms were assigned from bond valence and thermal factor considerations. Geometrical constraints were applied to localize hydrogen atoms of the amines (HFIX 137 option applied to N(1), C(1) and N(2), C(2)). The thermal factor of the oxygen atom $O_w$ of the water molecule being quite high, the hydrogen atoms were not imposed. All of the atoms were refined with an individual anisotropic thermal motion except the H atoms for which a common isotropic factor was imposed.

The atomic coordinates, the anisotropic displacement parameters, and the principal bond lengths and angles are given in Tables 2, 3, and 4, respectively.

**TABLE 2**
**Atomic Coordinates ($\times 10^4$, Except for Hydrogen Atoms $\times 10^3$) and Equivalent Isotropic Displacement Parameters (A$^2 \times 10^3$)**

| Atoms | $x$ | $y$ | $z$ | $U$ (eq) |
|---|---|---|---|---|
| Fe(1) | 7285(1) | 1823(1) | 3015(1) | 11(1) |
| Fe(2) | 0707(1) | 3492(1) | 2685(1) | 11(1) |
| Fe(3) | 5908(1) | 1510(1) | 961(1) | 11(1) |
| P(1) | 3772(1) | 1584(1) | 2443(1) | 11(1) |
| P(2) | 7874(1) | 3808(1) | 1586(1) | 10(1) |
| P(3) | 8917(1) | 3688(1) | 4316(1) | 11(1) |
| F(1) | 9513(1) | 1830(1) | 2844(1) | 16(1) |
| F(2) | 7055(1) | 894(1) | 1972(1) | 15(1) |
| O(1) | 5048(1) | 1829(1) | 3078(1) | 15(1) |
| O(2) | 9623(2) | 3655(1) | 1684(1) | 16(1) |
| O(3) | 7149(2) | 3420(1) | 2355(1) | 15(1) |
| O(4) | 9633(2) | 2974(1) | 5036(1) | 17(1) |
| O(5) | 8308(2) | 5023(1) | 4559(1) | 16(1) |
| O(6) | 7290(2) | 2932(1) | 890(1) | 15(1) |
| O(7) | 4261(2) | 1948(1) | 1609(1) | 16(1) |
| O(8) | 7603(2) | 2861(1) | 3972(1) | 15(1) |
| O(9) | 0132(2) | 3971(2) | 3707(1) | 20(1) |
| O(10) | 3234(2) | 170(1) | 2458(1) | 15(1) |
| O(11) | 7467(2) | 5210(1) | 1370(1) | 15(1) |
| O(12) | 2456(2) | 2484(1) | 2638(1) | 20(1) |
| O*W* | 4611(4) | 1519(5) | 4753(2) | 110(2) |
| N(1) | 7525(3) | 936(3) | 5450(2) | 61(1) |
| N(2) | 0123(2) | −220(2) | 1778(1) | 32(1) |
| C(1) | 1434(4) | 12(4) | 4204(2) | 50(1) |
| C(2) | 510(5) | 271(5) | 1006(2) | 69(1) |
| H(1*A*) | 658(1) | 65(2) | 548(2) | 123(7) |
| H(1*B*) | 773(3) | 106(3) | 495(1) | 123(7) |
| H(1*C*) | 763(3) | 168(1) | 571(2) | 123(7) |
| H(2*A*) | 1(4) | −107(1) | 175(1) | 123(7) |
| H(2*B*) | 927(3) | 14(3) | 192(1) | 123(7) |
| H(2*C*) | 086(2) | −3(4) | 213(1) | 123(7) |
| H(1*D*) | 042(1) | −32(2) | 421(2) | 123(7) |
| H(1*E*) | 169(3) | 18(3) | 367(1) | 123(7) |
| H(1*F*) | 150(3) | 79(1) | 451(1) | 123(7) |
| H(2*D*) | 130(3) | −25(2) | 80(1) | 123(7) |
| H(2*E*) | 85(4) | 115(1) | 106(1) | 123(7) |
| H(2*F*) | −37(1) | 24(4) | 65(1) | 123(7) |

## 3. Magnetic and Mössbauer Study

The magnetization $M$ of the sample was measured as a function of the applied field H (500 Gauss) at many temperatures in the range 4 to 300 K with a Quantum Design Squid device. The resulting magnetic susceptibility was deduced.

$^{57}$Fe Mössbauer spectra were recorded at 300, 78, 23, and 4.2 K using a constant acceleration spectrometer using a $^{57}$Co source diffused in a Rh matrix. The values of isomer shifts are quoted here relative to $\alpha$-Fe foil at 300 K. The hyperfine parameters were refined using a least-squares fitting procedure (13).

**TABLE 3**
**Anisotropic Displacement Parameters ($Å^2 \times 10^3$)**

| Atoms | U11 | U22 | U33 | U23 | U13 | U12 |
|---|---|---|---|---|---|---|
| Fe(1) | 10(1) | 9(1) | 10(1) | 0(1) | 0(1) | 1(1) |
| Fe(2) | 9(1) | 11(1) | 13(1) | 0(1) | 1(1) | 1(1) |
| Fe(3) | 12(1) | 10(1) | 11(1) | − 1(1) | − 1(1) | 0(1) |
| P(1) | 8(1) | 10(1) | 14(1) | 0(1) | 1(1) | 1(1) |
| P(2) | 12(1) | 9(1) | 10(1) | 0(1) | − 1(1) | − 1(1) |
| P(3) | 14(1) | 10(1) | 9(1) | 0(1) | − 1(1) | − 2(1) |
| F(1) | 10(1) | 14(1) | 24(1) | 1(1) | 2(1) | − 1(1) |
| F(2) | 19(1) | 14(1) | 13(1) | − 2(1) | − 2(1) | 2(1) |
| O(1) | 1(1) | 20(1) | 15(1) | − 1(1) | 1(1) | − 2(1) |
| O(2) | 12(1) | 22(1) | 15(1) | 2(1) | − 2(1) | − 1(1) |
| O(3) | 19(1) | 12(1) | 14(1) | 1(1) | 3(1) | 0(1) |
| O(4) | 22(1) | 15(1) | 14(1) | 3(1) | − 7(1) | − 3(1) |
| O(5) | 22(1) | 11(1) | 16(1) | 0(1) | 3(1) | − 1(1) |
| O(6) | 18(1) | 12(1) | 13(1) | − 2(1) | 0(1) | − 4(1) |
| O(7) | 14(1) | 19(1) | 15(1) | 3(1) | 2(1) | 2(1) |
| O(8) | 15(1) | 16(1) | 13(1) | − 3(1) | 0(1) | − 3(1) |
| O(9) | 19(1) | 26(1) | 15(1) | − 2(1) | 4(1) | − 9(1) |
| O(10) | 15(1) | 1(1) | 21(1) | − 1(1) | 1(1) | − 1(1) |
| O(11) | 20(1) | 9(1) | 15(1) | 0(1) | − 1(1) | 1(1) |
| O(12) | 13(1) | 17(1) | 30(1) | 0(1) | 5(1) | 6(1) |
| O*W* | 54(2) | 231(6) | 48(2) | 24(2) | 17(1) | 14(2) |
| N(1) | 46(2) | 53(2) | 81(2) | 30(2) | − 14(2) | − 14(1) |
| N(2) | 27(1) | 26(1) | 43(1) | 1(1) | 1(1) | 0(1) |
| C(1) | 50(2) | 53(2) | 47(2) | 2(1) | − 1(1) | 6(2) |
| C(2) | 51(2) | 127(4) | 30(2) | 11(2) | 0(1) | − 16(2) |

*Note.* The anisotropic displacement factor exponent takes the form $-2\Pi^2[h^2a^{*2}U_{11} + k^2b^{*2}U_{22} + \cdots + 2hka^*b^*U_{12} + \cdots]$.

## STRUCTURAL DESCRIPTION

$[Fe_3(PO_4)_3F_2, (CH_3NH_3)_2, H_2O]$ is a three-dimensional oxyfluorinated ferric phosphate (Fig. 1). The inorganic part of its structure is built up from the corner-sharing of hexameric units (Fig. 2a). These bricks contain one central octahedron $Fe(1)O_4F_2$, two trigonal bipyramids $Fe(2,3)O_4F$, and three $PO_4$ tetrahedra. The $PO_4$ tetrahedra cap the ferric trimer formed by the corner-sharing of the fluorine atoms present in the iron coordination polyhedra (Fig. 2b). The three-dimensional connection between ferric trimers is ensured by the $PO_4$ tetrahedra via oxygen vertices. Ten-membered tunnels in the [010] direction, in which methylamine and water molecules are inserted, are observed. Eight-membered channels along [100] also appear (Fig. 3). Strong hydrogen bonds exist between hydrogen atoms of the ammonium groups and oxygen atoms of the inorganic framework (O(1)–H(2*A*) = 2.198 Å, O(10)–H(2C) = 2.152 Å, O(7)–H(1C) = 2.492 Å). Water molecules are also located within the tunnels but, at variance to what was previously observed in ULM-3 (14), they are not strongly bonded to the amine (O*W*–H(1A) = 2.268 Å). That means that it is not, this time, the amine hydrate which acts as a template.

**TABLE 4**
**Principal Interatomic Distances (Å) and Angles (°)**

$Fe(1)O_4F_2$ octahedron

| Fe(1) | O(8) | O(11) | O(1) | O(3) | F(1) | F(2) |
|---|---|---|---|---|---|---|
| O(8) | **1.955(1)** | 2.811(1) | 2.865(1) | 2.810(1) | 2.825(1) | 3.965(1) |
| O(11) | 91.23(5) | **1.977(1)** | 2.885(1) | 3.974(1) | 3.990(1) | 2.907(1) |
| O(1) | 93.22(5) | 93.38(6) | **1.987(1)** | 2.812(1) | 3.991(1) | 2.818(1) |
| O(3) | 90.58(6) | 176.29(6) | 89.76(6) | **1.998(1)** | 2.759(1) | 2.700(1) |
| F(1) | 90.94(5) | 89.71(5) | 174.76(5) | 87.02(5) | **2.007(1)** | 2.745(1) |
| F(2) | 174.39(5) | 93.49(5) | 89.53(5) | 84.53(5) | 86.06(5) | **2.015(1)** |

$\langle Fe(1)–O\rangle = 1.979(1)$ Å $\quad \langle Fe(1)–F\rangle = 2.011(1)$ Å

$Fe(2)O_4F$ trigonal bipyramid

| Fe(2) | O(12) | O(9) | O(2) | O(10) | F(1) |
|---|---|---|---|---|---|
| O(12) | **1.873(1)** | 3.204(1) | 3.157(1) | 2.855(1) | 2.731(1) |
| O(9) | 116.45(7) | **1.897(1)** | 3.451(1) | 2.797(1) | 2.700(1) |
| O(2) | 112.95(6) | 129.88(6) | **1.914(1)** | 2.811(1) | 2.734(1) |
| O(10) | 95.05(6) | 91.77(6) | 91.91(6) | **1.997(1)** | 4.043(1) |
| F(1) | 88.19(5) | 86.36(5) | 87.24(5) | 176.73(5) | **2.047(1)** |

$\langle Fe(2)–O\rangle = 1.920(1)$ Å $\quad \langle Fe(2)–F\rangle = 2.047(1)$ Å

$Fe(3)O_4F$ trigonal bipyramid

| Fe(3) | O(7) | O(5) | O(6) | O(4) | F(2) |
|---|---|---|---|---|---|
| O(7) | **1.922(1)** | 3.600(1) | 3.168(1) | 2.704(1) | 2.745(1) |
| O(5) | 138.81(6) | **1.923(1)** | 3.150(1) | 2.825(1) | 2.751(1) |
| O(6) | 110.92(6) | 109.93(6) | **1.924(1)** | 2.858(1) | 2.813(1) |
| O(4) | 88.30(6) | 93.38(6) | 94.80(6) | **1.959(1)** | 4.004(1) |
| F(2) | 87.37(5) | 87.57(5) | 90.05(5) | 174.41(6) | **2.050(1)** |

$\langle Fe(3)–O\rangle = 1.932(1)$ Å $\quad \langle Fe(3)–F\rangle = 2.050(1)$ Å

$P(1)O_4$ tetrahedron

| P(1) | O(12) | O(1) | O(10) | O(7) |
|---|---|---|---|---|
| O(12) | **1.541(1)** | 2.471(1) | 2.520(1) | 2.486(1) |
| O(1) | 106.59(8) | **1.542(1)** | 2.544(1) | 2.554(1) |
| O(10) | 109.57(8) | 111.14(8) | **1.543(1)** | 2.535(1) |
| O(7) | 107.30(8) | 111.69(7) | 110.39(8) | **1.545(1)** |

$\langle P(1)–O\rangle = 1.543(1)$ Å

$P(2)O_4$ tetrahedron

| P(2) | O(3) | O(11) | O(6) | O(2) |
|---|---|---|---|---|
| O(3) | **1.536(1)** | 2.521(1) | 2.543(1) | 2.529(1) |
| O(11) | 110.27(7) | **1.538(1)** | 2.502(1) | 2.534(1) |
| O(6) | 110.67(7) | 107.92(7) | **1.556(1)** | 2.521(1) |
| O(2) | 109.76(8) | 110.00(8) | 108.18(8) | **1.556(1)** |

$\langle P(2)–O\rangle = 1.546(1)$ Å

$P(3)O_4$ tetrahedron

| P(3) | O(4) | O(8) | O(5) | O(9) |
|---|---|---|---|---|
| O(4) | **1.536(1)** | 2.484(1) | 2.540(1) | 2.537(1) |
| O(8) | 107.88(8) | **1.536(1)** | 2.519(1) | 2.576(1) |
| O(5) | 110.84(8) | 109.45(8) | **1.550(1)** | 2.473(1) |
| O(9) | 110.28(8) | 112.88(7) | 105.53(8) | **1.556(1)** |

$\langle P(3)–O\rangle = 1.554(1)$ Å

*Note.* Distances in methylamine molecules: N(1)–C(1): 1.451(4) Å; N(2)–C(2): 1.461(4) Å.

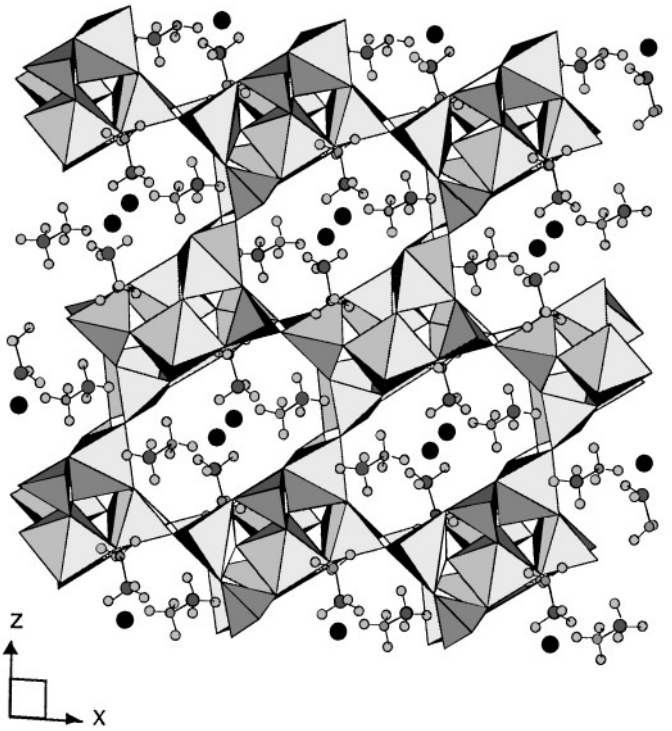


**FIG. 1.** Projection of the structure of $[Fe_3(PO_4)_3F_2, (CH_3NH_3)_2, H_2O]$ along [010]. Water (black circles) and methylamine molecules are inserted in the 10-membered channels.

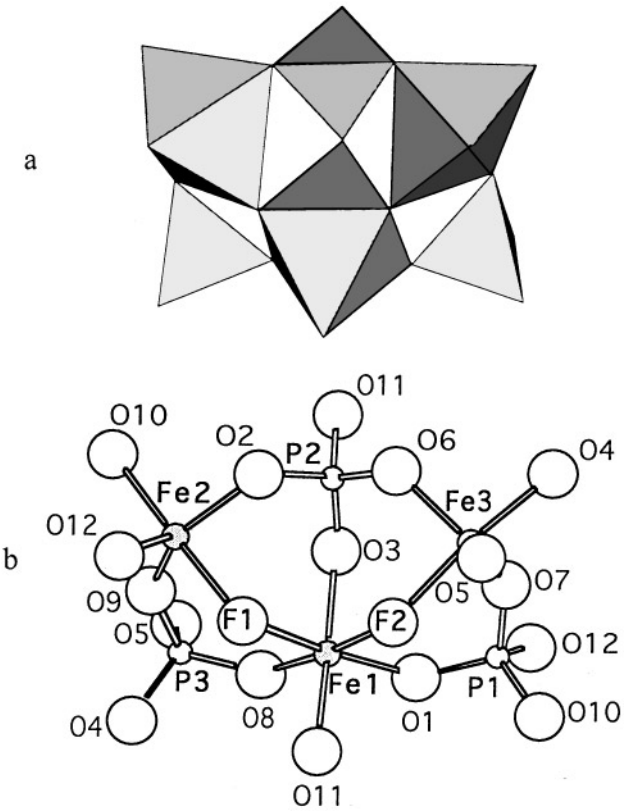


**FIG. 2.** A hexameric brick: (a) polyhedral representation, (b) balls and sticks representation with labeled atoms.

The thermogravimetric curve of $[Fe_3(PO_4)_3F_2, (CH_3NH_3)_2, H_2O]$ indicates two distinct weight losses (Fig. 4). The first occurring at about 100°C, corresponds to the dehydration of the compound ($\%_{theo} = 3.1$, $\%_{exp} = 3$); the second loss at ca 330°C fits with the departure of the amines and H*F* ($\%_{theo} = 17.8\%$, $\%_{exp} = 17.7$). After this thermal treatment, the residue is amorphous.

As mentioned above, $[Fe_3(PO_4)_3F_2, (CH_3NH_3)_2, H_2O]$ is isostructural with the gallophosphate ULM-4 or $[Ga_3(PO_4)_3F_2, (CH_3NH_3)_2, H_2O]$ (15). According to Shannon (16), the calculated distortion $\Delta$ of each iron coordination polyhedron

$$(\Delta = \frac{1}{i}\sum_i \left[\frac{x_i - \bar{x}}{\bar{x}}\right]^2$$

with $x_i$ equal to the distance between the central cation and anion $i$, $\bar{x}$ equal to the average anion–cation distance) indicates that the two fivefold-coordinated Fe(III) are more distorted than the central octahedron: $10^4.\Delta = 11.4$ for $Fe(2)O_4F$, $10^4.\Delta = 6.3$ for $Fe(3)O_4F$, and $10^4.\Delta = 0.8$ for $Fe(1)O_4F_2$. Compared with the gallophosphate, in both cases the central octahedra are quite regular, but external trigonal bipyramids are more distorted in the gallophosphate than in the iron phosphate. We already observed the same phenomena between the gallophosphate ULM-3 (14) and its iron homologue (9).

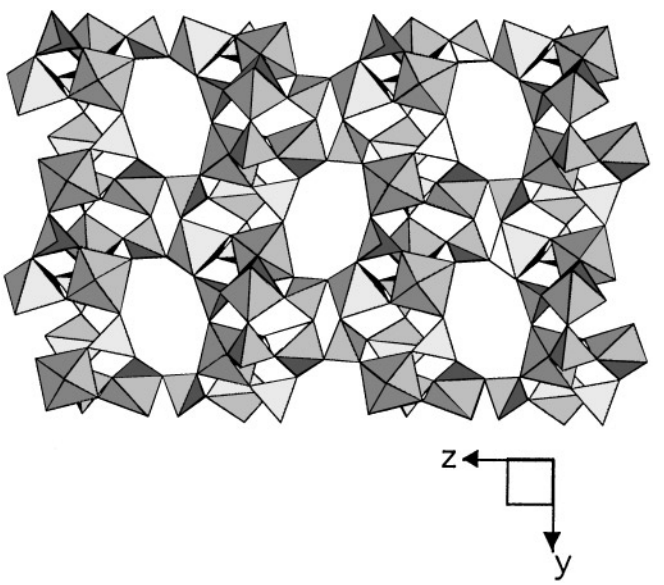


**FIG. 3.** [100] projection of the structure of $[Fe_3(PO_4)_3F_2, (CH_3NH_3)_2, H_2O]$ showing the 8-membered channels.

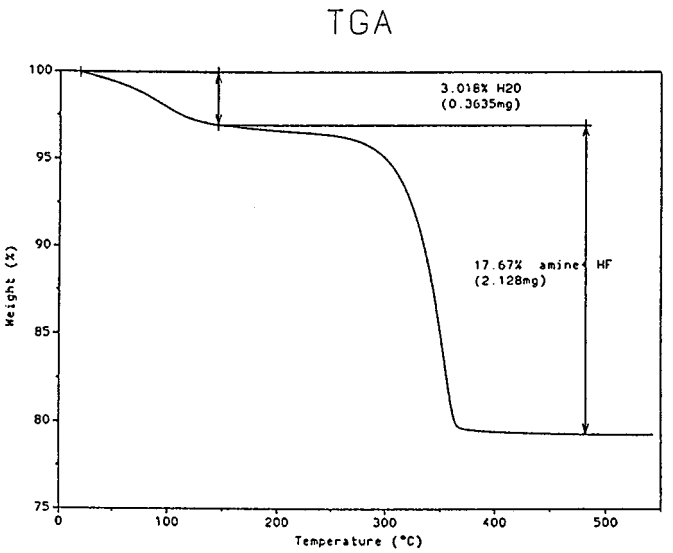


**FIG. 4.** Thermogravimetric curve of $[Fe_3(PO_4)_3F_2, (CH_3NH_3)_2, H_2O]$ under $O_2$ atmosphere.

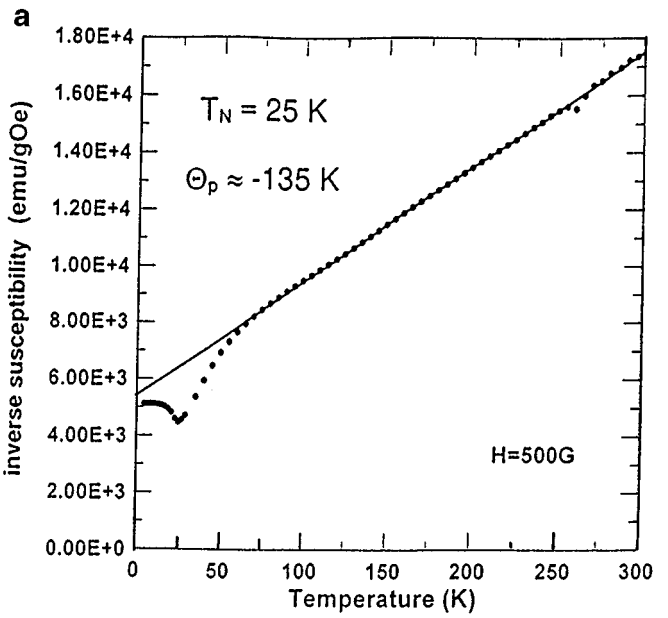


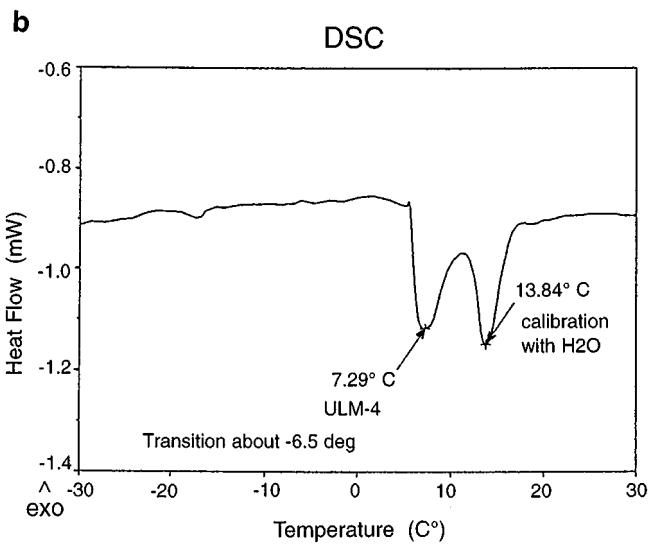


**FIG. 5.** (a) Thermal variation of the inverse magnetic susceptibility of $[Fe_3(PO_4)_3F_2, (CH_3NH_3)_2, H_2O]$; (b) The DSC endothermic effect is presented (1st peak), the 2nd peak corresponds to water (a pseudo-calibration with pure water was made and confirmed this second point).

## MAGNETIC AND MÖSSBAUER STUDIES

### *1. Magnetic Susceptibility*

The thermal variation of the inverse magnetic susceptibility of $[Fe_3(PO_4)_3F_2, (CH_3NH_3)_2, H_2O]$ is represented in Fig. 5a. It is characteristic of a canted antiferromagnetic compound (the magnetic moments are not perfectly antiparallel and lead to a small ferromagnetic component). The Néel temperature $T_N$ is 25(1) K; the asymptotic Curie–Weiss temperature $\theta_p = -135$ K reveals predominant antiferromagnetic interactions in the compound. However, the $|\theta_p/T_N|$ ratio widely exceeds unity and is consistent with the presence of magnetic frustration in $[Fe_3(PO_4)_3F_2, (CH_3NH_3)_2, H_2O]$. The experimental effective moment of a $Fe^{3+}$ ion is nearly 6.2(3) μB (a bit larger than the theoretical moment 5.9 μB). A reproducible slight accident is observed at ca 265 K on the $\chi^{-1}(T)$ curve. A DSC study shows that it corresponds to a weak endothermic effect (Fig. 5b); therefore, it may be attributed to a crystalline phase transition whose study is currently in progress.

### *2. Mössbauer Results of* $[Fe_3(PO_4)_3F_2, (CH_3NH_3)_2, H_2O]$

Some of the Mössbauer spectra recorded in the paramagnetic and in the magnetic range are illustrated in Figs. 6a and 6b, respectively. The weakly asymmetric quadrupolar doublets and magnetic sextets both exhibit rather narrow lines. Mössbauer spectra were fitted with three components assuming (i) the equiprobability of finding the three $Fe^{3+}$ sites, in agreement with the crystallographic data, and (ii) the same values of isomer shift for the two fivefold-coordinated $Fe^{3+}$ sites. In this way, the spectra are well fitted and the temperature dependence of the refined values of the hyperfine parameters is physically realistic. These values are listed in Tables 5 and 6.

In the paramagnetic state (Table 5), the isomer shift values are consistent with high spin state $Fe^{3+}$ located either in octahedral units for $\Gamma_1$ or in trigonal bipyramids for $\Gamma_2$ and $\Gamma_3$. We can attribute the two components $\Gamma_2$ and $\Gamma_3$ to Fe(2) and Fe(3) respectively taking into account the distortion of the trigonal bipyramids. Indeed, the higher the

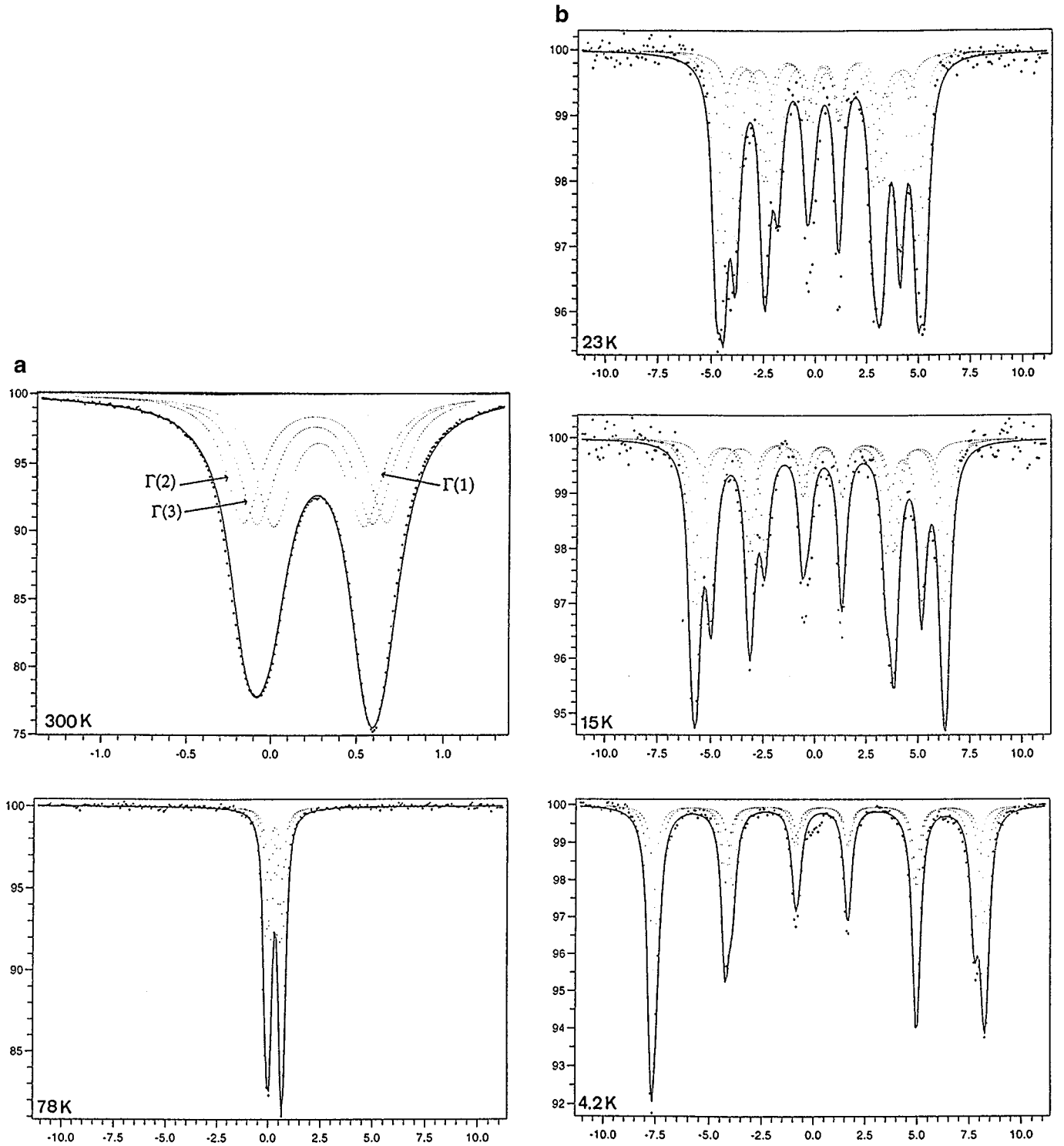


**FIG. 6.** Mössbauer spectra recorded (a) in the paramagnetic state (300 and 78 K) with the correlation with the three different crystallographic sites and (b) in the magnetic state (23, 15, and 4.2 K).

distortion of the polyhedron, the larger is the quadrupolar splitting (17). The low values of the linewidths indicate a well-crystallized state.

In the magnetic state (Table 6), below 25 K, the isomer shift values confirm the assignment of $Fe^{3+}$ in octahedral and bipyramidal sites made in the paramagnetic range.

**TABLE 5**
**Hyperfine Parameters in the Paramagnetic State Relative to α-Fe Foil at 300 K**

| | | IS mm/s | GA mm/s ± 0.02 | QS mm/s ± 0.02 | % |
|---|---|---|---|---|---|
| 300 K | Γ1 | 0.40 | 0.13 | 0.53 | 33.33 |
| | Γ2 | 0.38 | 0.13 | 0.84 | 33.33 |
| | Γ3 | 0.38 | 0.13 | 0.68 | 33.33 |
| 78 K | Γ1 | 0.46 | 0.14 | 0.48 | 33.33 |
| | Γ2 | 0.44 | 0.14 | 0.92 | 33.33 |
| | Γ3 | 0.44 | 0.14 | 0.66 | 33.33 |

*Note.* Γ*i*, component *i*; IS, isomer shift; GA, linewidth at halfheight; QS, quadripolar splitting; %, ratio of each component.

Moreover, in spite of different coordination states, the values of the hyperfine fields at 4.2 K are very similar. These values can be compared to those encountered in other ULM-*n* phases such as ULM-3 (49–51 T range at 4.2 K) (9); however, the values of the hyperfine fields at saturation are rather low in comparison with those expected for high spin state $Fe^{3+}$ ions in octahedral coordination ($H_{hyp} = -25$ T per spin unity, that is to say $H_{hyp}^{sat} = -62.5$ T). This lowering may be attributed to the presence of (i) oxygen ligands which are less effective than fluorine ligands in superexchange interactions ($H_{hyp}$(*r*-$FeF_3$) = − 61.8 T (18), $H_{hyp}$ (α-$Fe_2O_3$) = − 54.4 T (19)); or (ii) magnetic frustration which originates from the competition between strong antiferromagnetic superexchange interactions (through the *F* bridging ligand) within the ferric trimer and supersuperexchange interactions (through bridging $PO_4$ tetrahedral units). Such situations were previously found and extensively discussed in several iron-based ULM phases such as ULM-3 (9) and ULM-12 (5). However, such a discussion cannot be undertaken here since the low-temperature structure ($T < 260$ K) is not solved. Mössbauer study shows however that, after the transition, the coordination of Fe(III) ions are preserved. The resolution of the structure of the *LT* phase and the magnetic structure of the title compound are currently in progress.

**TABLE 6**
**Hyperfine Parameters in the Magnetic State**

| | | IS mm/s | GA mm/s ± 0.02 | 2ε mm/s ± 0.02 | $H_{hyp}$ (T) ± 0.5 |
|---|---|---|---|---|---|
| 23 K | Γ1 | 0.46 | 0.25 | − 0.109 | 31.3 |
| | Γ2 | 0.44 | 0.25 | − 0.077 | 29.1 |
| | Γ3 | 0.44 | 0.25 | − 0.367 | 24.7 |
| 15 K | Γ1 | 0.46 | 0.21 | − 0.078 | 44.5 |
| | Γ2 | 0.44 | 0.21 | − 0.220 | 44.4 |
| | Γ3 | 0.44 | 0.21 | − 0.423 | 39.7 |
| 4.2 K | Γ1 | 0.46 | 0.21 | − 0.042 | 49.9 |
| | Γ2 | 0.44 | 0.21 | − 0.162 | 49.4 |
| | Γ3 | 0.44 | 0.21 | − 0.357 | 47.4 |

*Note.* Γ*i*, component *i*; IS, isomer shift; GA, linewidth at halfheight; 2ε, quadripolar shift; $H_{hyp}$, hyperfine field.


## ACKNOWLEDGMENT

The authors are very indebted to Dr. Didier Riou (Institut Lavoisier, Versailles) for the X-ray data collection.


## REFERENCES


1. R. C. Haushalter and L. A. Mundi, *Chem. Mater.* **4,** 31 (1992).
2. V. Soghomonian, Q. Chen, R. C. Haushalter, J. Zubieta, C. J. O'Connor, and Y. S. Lee, *Chem. Mater.* **5,** 1690 (1993).
3. J. Chen, R. H. Jones, S. Natarajan, M. B. Hursthouse, and J. M. Thomas, *Angew. Chem.* **33,** 639 (1994).
4. M. Cavellec, D. Riou, and G. Férey, *J. Solid State Chem.* **112,** 441 (1994).
5. M. Cavellec, D. Riou, C. Ninclaus, J. M. Grenèche, and G. Férey, *Zeolites* **17,** 250 (1996).
6. M. Cavellec, D. Riou, J. M. Grenèche, and G. Férey, *Microporous Mater.* **8,** 103 (1997).
7. G. Férey, *J. Fluorine Chem.* **72,** 187 (1995).
8. D. Riou and G. Férey, *J. Solid State Chem.* **111,** 422 (1994).
9. M. Cavellec, D. Riou, J. M. Grenèche, and G. Férey, *J. Magn. Magn. Mater.* **163,** 173 (1996).
10. M. Cavellec, D. Riou, and G. Férey, *Eur. J. Solid State Inorg. Chem.* **32,** 271 (1995).
11. J. R. D. DeBord, W. M. Reiff, C. J. Warren, R. C. Haushalter, and J. Zubieta, private communication, 1997.
12. K.-H. Lii and Y-F. Huang, *Chem. Commun.* 839 (1997). [and preprints]
13. J. Teillet and F. Varret, "MOSFIT" program, unpublished.
14. T. Loiseau, R. Retoux, P. Lacorre, and G. Férey, *J. Solid State Chem.* **111,** 427 (1994); T. Loiseau, F. Taulelle, and G. Férey, *Microporous Mater.* **5,** 365 (1996).
15. M. Cavellec, D. Riou, and G. Férey, *Eur. J. Solid State Inorg. Chem.* **31,** 583 (1994).
16. R. D. Shannon, *Acta Crystallogr. A* **32,** 751 (1976).
17. N. N. Greenwood and T. C. Gibb, *in* "Mössbauer Spectroscopy." Chapman and Hall, London, 1971.
18. G. K. Wertheim, H. J. Guggenheim, and D. N. E. Buchanan, *Phys. Rev.* **169,** 465 (1968).
19. F. Van der Woude, *Phys. Status Solidi* **253,** 1253 (1966).